Journal of Experimental Botany, Vol. 69, No. 21 pp. 5177–5189, 2018
doi:10.1093/jxb/ery299 Advance Access publication 22 August 2018

RESEARCH PAPER

Dual functions of ZmNF-YA3 in photoperiod-dependent flowering and abiotic stress responses in maize

Huihui Su[1,*], Yingying Cao[1,*], Lixia Ku[1,*,†], Wen Yao[1], Yanyong Cao[2], Zhenzhen Ren[1], Dandan Dou[1], Huitao Wang[1], Zhaobin Ren[1], Huafeng Liu[1], Lei Tian[1], Yaogang Zheng[1], Chen Chen[1], and Yanhui Chen[1,†]

[1] Synergetic Innovation Centre of Henan Grain Crops and National Key Laboratory of Wheat and Maize Crop Science, Henan Agricultural University, Zhengzhou 450002, China
[2] Henan Academy of Agricultural Science, Zhengzhou, Henan, 450002, China

* These authors contributed equally to this work.

† Correspondence: chy9890@163.com or kulixia0371@163.com

Received 9 March 2018; Editorial decision 6 August 2018; Accepted 16 August 2018

Editor: Dabing Zhang, Shanghai Jiao Tong University, China

Abstract

Nuclear factor-Y (NF-Y) transcription factors are important regulators of several essential biological processes, including embryogenesis, drought resistance, meristem maintenance, and photoperiod-dependent flowering in Arabidopsis. However, the regulatory mechanisms of NF-Ys in maize (*Zea mays*) are not well understood yet. In this study, we identified an NF-Y transcription factor, ZmNF-YA3. Genome-wide analysis showed that ZmNF-YA3 bound to >6000 sites in the maize genome, 2259 of which are associated with genic sequences. ZmNF-YA3 was found to interact with CONSTANS-like (CO-like) and flowering promoting factor1 (FPF1) through yeast two-hybrid and bimolecular fluorescence complementation (BiFC) assays. Quantitative real-time reverse transcription–PCR (qRT–PCR) combined with yeast one-hybrid assay and EMSA suggested that NF-YA3 could promote early flowering by binding to the FLOWERING LOCUS T-like12 (FT-like12) promoter in maize. Morerover, we also showed that ZmNF-YA3 could improve drought and high-temperature tolerance through binding to the promoter regions of bHLH92, FAMA, and the jasmonic acid activator MYC4, respectively. These results contribute to a comprehensive understanding of the molecular mechanisms and regulatory networks of NF-Y transcription factors in regulating maize flowering time and stress response in maize.

Keywords: CHIP-Seq, maize, photoperiod, qRT–PCR, regulatory pathway, stress tolerance.

Introduction

Nuclear factor-Y (NF-Y) transcription factors (TFs) are known to bind specifically to a highly conserved CCAAT sequence in promoter regions of their target genes (Romier *et al.*, 2003; Frontini *et al.*, 2004; Steidl *et al.*, 2004). All NF-Ys share conserved domains required for DNA binding and protein interactions (Romier *et al.*, 2003; Laloum *et al.*, 2013). DNA-binding domains of NF-Ys are heterotrimeric complexes composed of three unique subunits, NF-YA (HAP2), NF-YB (HAP3), and NF-YC (HAP5), which are conserved from yeast to mammals. However, all three NF-Y families have undergone an expansion in plants, with most species encoding ~10 genes per family (Petroni *et al.*, 2012; Laloum *et al.*, 2013). Because NF-Y binds to DNA as a heterotrimer, ~1000 different NF-Ys could be formed (Petroni *et al.*, 2012). These complexes greatly diversify the regulation of multiple important plant processes, such as the abscisic acid (ABA) signalling

pathway, photoperiod-dependent flowering, root development, embryogenesis, nodule development, and stress responses (Ben-Naim *et al.*, 2006; Wenkel *et al.*, 2006; Nelson *et al.*, 2007; Kumimoto *et al.*, 2010; Ballif *et al.*, 2011; Kumimoto *et al.*, 2013; Mu *et al.*, 2013; Lee *et al.*, 2015; Siriwardana *et al.*, 2016).

Many studies have shown that NF-Ys play important roles in flowering regulation. In Arabidopsis, CONSTANS (CO) interacts with the NF-YB and NF-YC subunits *in vivo*, forming complexes to regulate *FLOWERING LOCUS T* (*FT*), then initiating the downstream events leading to the floral transition (Ben-Naim *et al.*, 2006; Wenkel *et al.*, 2006; Kumimoto *et al.*, 2008, 2010; Hou *et al.*, 2014). NF-Ys may also negatively regulate flowering time based on the fact that overexpression of some *NF-YA* genes can cause late flowering (Wenkel *et al.*, 2006; Xu *et al.*, 2014). NF-YA and CO proteins share a region of sequence homology; they may compete for the occupancy of NF-YB/C dimers. On the other hand, Siriwardana *et al.* (2016) showed that NF-YA, in complex with NF-YB and NF-YC proteins, can directly bind to the distal CCAAT box in the FT promoter and is a positive regulator of flowering in an FT-dependent manner in Arabidopsis. However, whether NF-YA proteins are regulators of photoperiod-dependent flowering and whether this regulation is dependent on CO or FT are essential questions that need to be well studied.

NF-Ys were also identified to be involved in abiotic stress responses. In both maize (*Zea mays*) and Arabidopsis, the overexpression of NF-YB1 and NF-YB2, respectively, promotes drought resistance (Nelson *et al.*, 2007). Leyva-González *et al.* (2012) found that the overexpression of NF-YA members affected tolerance to diverse abiotic stresses, including drought, logging, cold, and heat, and sequestering the NF-YB/NF-YC heterodimers could prevent their interactions with other TFs that induce the expression of stress-responsive genes in Arabidopsis. The NF-YA subunit plays essential roles in ABA-mediated response, where ABA is perceived through the pyrabactin resistance1 components of the ABA receptor family of soluble receptors in Arabidopsis (Fujii *et al.*, 2009; Miyazono *et al.*, 2009). The association of ABA with pyrabactin resistance1 initiates a signalling cascade through PP2C phosphatases and SnRK2 kinases to activate basic leucine zipper (bZIP) TFs that bind ABA response elements in the promoters of ABA response genes in Arabidopsis (Fujii *et al.*, 2009).

In conclusion, NF-Ys are shown to regulate photoperiod-dependent flowering time and stress responses in Arabidopsis. However, the molecular bases of NF-Ys in flowering time regulation and stress response still remain unknown in maize. In our previous study, a set of differentially expressed genes were found to affect flowering time and biotic and abiotic stresses through a transcriptome analysis by utilizing HZ4-NIL (photoperiod-sensitive lines) and HZ4 (photoperiod-insensitive lines) under long-day (LD) conditions (Ku *et al.*, 2016), and NF-YA3 (GRMZM2G040349) is one of them. In this study, we used NF-YA3 to study the regulatory mechanism of photoperiod-dependent flowering time and stress responses. We demonstrated that NF-YA3 firstly interacts with CO-like and flowering promoting factor1 (FPF1) to form complexes, and then binds to the promoter region of ZmFT-like12 (–3109 bp) to promote early flowering. Meanwhile, ZmNF-YA3 confers drought stress tolerance in an ABA-dependent manner by binding to the promoters of bHLH92 and FAMA (FMA), and improves abiotic stress tolerance by binding to the promoter of the jasmonic acid (JA) activator MYC4 through the JA-induced signalling pathway in maize. Thus, ZmNF-YA3 plays important roles in the regulation of photoperiod-dependent flowering time and drought stress tolerance in maize.

Materials and methods

Plant materials

The ZmNF-YA3 and ZmFT-like12 knock-out mutants were obtained using the CRISPR–Cas9 (clustered regularly interspaced short palindromic repeats–CRISPR-associated protein9)-mediated mutagenesis system (Xing *et al.* 2014). Guide RNAs (gRNAs; targeting sequences) were selected by using the online tool CRISPR-PLANT (http://www.genome.arizona.edu/crispr/CRISPRsearch.html) and all the gRNAs are listed in Supplementary Table S1 at *JXB* online. We followed the vector construction protocol as previously described in Xing *et al.* (2014); therefore, the gRNAs were constructed into the pBUE411vector. The immature zygotic embryos from maize inbred line Yu658 were harvested ~9 d after pollination and used for *Agrobacterium*-mediated transformation following previous protocols (Frame *et al.*, 2002). In short, the immature embryos were infected by *Agrobacterium* for 5 min, and then placed on the co-cultivation medium at 18 °C for 3 d in the dark. After that, embryos were transferred to resting medium at 28 °C in the dark for 7 d and then transferred to selection medium I for 2 weeks with the same conditions as on the resting medium. Additionally, they were subcultured on selection medium II for 4–6 weeks. The putative transformed calli were harvested and then regenerated for three 2 week subculture steps in pre-regeneration medium (dark), regeneration medium I (dark), and regeneration medium II (light) at 28 °C, respectively.

The mutants, Zmft-like12 and Zmnf-ya3, were obtained from T_2 plant lines, and plants without any sequence editing were selected as the wild type (WT) (see Supplementary Fig. S1).

Monoclonal antibody and western blot analysis

To generate NF-YA3 antibody, a full-length NF-YA3 cDNA was cloned from leaf7 of Yu658 at the V7 stage using the primers shown in Supplementary Table S1 and then into the *Bgl*II and *Hin*dIII sites of the pET-28a(+) vector (Cat. JR136105 Novagen), and the construct was transformed into Rosetta (DE3) competent cells. Cells were grown at 37 °C and induced by the addition of isopropyl-β-D-thiogalactopyranoside to a final concentration of 1 mM when the optical density at 600 nm was 0.6. ZmNF-YA3 fused to 6× His was purified using a HisTrapTM FF crude column (Code No. 95056-156, GE Healthcare). Eluted proteins were boiled in 30 µl of 2× SDS buffer and then loaded onto an SDS–polyacrylamide gel for further analysis. The monoclonal antibody was produced in mice according to standard protocols of Shanghai ImmunoGen Biological Technology Co. Ltd. Total protein was extracted using a Tris–HCl procedure (Wu *et al.*, 2014) and the western blot analysis was performed according to the same method as described by Hirano (2012).

ChIP

ChIP with ZmNF-YA3 antibody was performed as previously published (Kaufmann *et al.*, 2010). Leaf7 from Yu658 at the V7 stage was obtained, and 3 g of sample was cross-linked in cross-linking buffer (25 ml) with 1% formaldehyde on ice under vacuum. The vacuum was released after 15 min and reapplied for another 14 min. Fixation was stopped by adding glycine to a final concentration of 0.125 M. The fixed sample was washed three times with sterile water and ground into powder in liquid nitrogen. Nuclear components were isolated by adding the frozen powder to 30 ml of M1 buffer. The homogenate was filtered through four layers of Miracloth prior to isolation of nuclei. Nuclear-enriched

extracts were resuspended in 5 ml of lysis buffer (50 mM HEPES, pH 7.5, 150 mM NaCl, 1 mM EDTA, 1% Triton X-100, 0.1% deoxycholate, 0.1% SDS, 1 mM phenylmethylsulphonyl fluoride, and 10 mM sodium butyrate) containing a plant proteinase inhibitor cocktail (Sigma-Aldrich, St. Louis, MO, USA), followed by sonication for 5 min on medium power in 1.5 ml of sonication buffer using a Bioruptor UCD-200 (Diangenode, Liege, Belgium). The chromatin solution was sonicated for 5 min on medium power five times to create ~400 bp average fragment sizes, as estimated by agarose gel electrophoresis. An antibody against NF-YA3 was used for immunoprecipitation, and the input served as the control. The precipitated DNA was recovered using a QIAquick PCR purification kit (Qiagen, Hilden, Germany).

ChIP DNA samples were subjected to end repair and A-base addition, followed by ligation with adaptors. Illumina Genome Analyzer sequencing was performed by the OSUCCC Nucleic Acid Shared Resource-Illumina Genome Analyzer II Core.

ChIP-Seq data analysis

We defined target genes as those that contained ChIP-Seq peaks located within the transcribed regions of genes, in introns or 5 kb upstream of the transcription start site (TSS), or 5 kb downstream of the transcription termination site (TTS). ChIP-Seq reads were aligned to the maize genome using Bowtie 2 (Langmead *et al.*, 2009). Bowtie 2 supports gapped and paired-end alignment modes. We ran Bowtie version 2.2.3 with default parameters and reported only unique alignments. ChIP-Seq peaks were detected by MACS2 (Zhang *et al.*, 2008). We used MACS version 2.0.10 with default parameters, as duplicates were allowed, and the q-value <0.05.

Electrophoretic mobility shift assay

The full-length NF-YA3 cDNA was amplified with gene primers (Supplementary Table S1) and fused into the *Sgf*I and *Pme*I sites of pFN19K Halo Tag® T7 SP6 Flexi® Vector. The Halo Tag-NF-YA3 fusion protein was expressed using TNT® Coupled Wheat Germ Extract Systems (Promega, Fitchburg, WI, USA) and Magne® Halo Tag Beads (Promega) for EMSA. Oligonucleotide probes (Supplementary Table S1) were synthesized and labelled according to the standard protocol of Invitrogen Technology (Shanghai, China). We used standard reaction mixtures for EMSA containing 20 ng of purified NF-YA3 fusion protein, 5 ng of biotin-labelled annealed oligonucleotides, 2 µl of 10× binding buffer (100 mM Tris, 500 mM KCl, and 10 mM DTT, pH 7.5), 1 µl of 50% (v/v) glycerol, 1 µl of 100 mM$MgCl_2$, 1 µl of 1 mg ml^{-1} poly(dI–dC), 1 µl of 1% (v/v) Nonidet P-40, and double-distilled water to a final volume of 20 µl. The reactions were incubated at 25 °C for 20 min, electrophoresed in 6% (w/v) polyacrylamide gels, and then transferred to N+ nylon membranes (Millipore, Darmstadt, Germany) in 0.53× TBE (Tris–Borate–EDTA) buffer at 380 mA at 4 °C for 30 min. Biotin-labelled DNA was detected using the LightShift™ Chemiluminescent EMSA kit (Thermo Fisher). Bands were visualized by the Chemiluminescent Western Blot Detection Kit (Thermo Fisher).

Yeast one-hybrid assays

Yeast one-hybrid (Y1H) assays were performed according to the Matchmaker Y1H system manufacturer's instructions (Clontech, Mountain View, CA, USA). Full-length ORFs of NF-YA3 were cloned into pGADT7 vector (Clontech); normal and mutant ~200 bp DNA fragments from TFIIIA, ATL6, MIF2, RPP13, MYB61, MYB4, FBX356, UVR3, CYP71A22, SAVR52, FT, MYC4, bHLH92, FMA, and bZIP45 promoters (the 100 bp flanking sequences around the genes of genic peak summits; Supplementary Table S3) were independently cloned into the pAbAi vector (Clontech) to generate reporter plasmids. The fusion pAbAi vectors were transformed into the Y1H Gold strain provided by Clontech and selected on synthetic dextrose (SD)/–Ura media. Then, the pAD7-NF-YA3 vector was transformed into 'Y1H Gold' with the fusion pAbAi vector. 'Y1H Gold' containing the pAD7-NF-YA3 vector was observed on selective SD plates without Leu plus Aureobasidin A (AbA★) (SD/–Leu/AbA★). p53HIS2 acted as a positive control, and the mutant ~200 bp DNA fragments (Supplementry Table S3) from the above genes using the Quick-Change site-directed mutagenesis kit (Stratagene, La Jolla, CA, USA) acted as negative controls. The mutant ~200 bp DNA fragments from the promoters of target genes were the sequences in the normal ~200 bp DNA fragments from which the motifs were deleted ; the deleted sequences are shown in red and underlined in Supplementary Table S3. All of the primer information of the generated constructs is shown in Supplementary Table S1.

Yeast two-hybrid and BiFC

For the yeast two-hybrid (Y2H) analysis, NF-YA3 cDNA was cloned into plasmid pGADT7 (pGADT7-NF-YA3). The full-length *CO-like* and *FPF1* cDNAs were independently cloned into the pGBKT7 plasmid (pGBKT7-CO-like and pGBKT7-FPF1). pGADT7-NF-YA3, pGBKT7-CO-like, and pGBKT7-FPF1 were transformed according to the manufacturer's instructions for the Matchmaker Gold Yeast Two-Hybrid System (Clontech). The primers used for the derived constructs are listed in Supplementary Table S1.

For the bimolecular fluorescence complementation (BiFC) experiment, NF-YA3, CO-like, or FPF1 was expressed as an in-frame fusion to the N- or C-terminus of yellow fluorescent protein (YFP; pSAT-nEYFP-C1 and pSAT-cEYFP-C1). Protoplasts were generated from 1-week-old Arabidopsis Col-0 suspension cell cultures as previously described (Walter *et al.*, 2004). Cells were collected by centrifugation at 400 *g* for 5 min and pellets were washed with 25 ml of cell wall digestion buffer lacking the digestion enzymes. Protoplasts were prepared and transformed according to previous protocols (Merkle *et al.*, 1996; Merkle and Nagy, 1997). Protoplasts were assayed for fluorescence 12–18 h after each co-transformation.

Experimental treatments

Treatments under long-day (LD) conditions

The Zmnf-ya3 mutant, Zmft-like12 mutant, and WT plants were grown in growth chambers (GR 64, Conviron, Canada). LD treatment involved, 15 h (06.00–19.00 h), light intensity 100 µmol m^{-2} s^{-1}, day temperature 28 °C, night temperature 22 °C, relative humidity 40%; short-day (SD) treatment involved, 9 h (06.00–15.00 h); other parameters were the same as for the LD treatment. In the present study, leaf blade tissue was collected from the V6, V7, V8, and V9 stage seedlings to analyse the expression levels of *ZmNF-YA3*, *ZmCO-like*, *ZmFPF1*, and *ZmFT-like12*. Each sample was collected from three different, randomly selected plants. Three biological replicates were collected at the same time. For shoot apical meristem (SAM) experiments, 15 seedlings were harvested separately in the V6 stage from Zmnf-ya3 mutant, Zmft-like mutant, and WT plants grown under LD conditions. Following previously described procedures (Li and Huang, 2005), first, the maize stem tips were fixed with FAA and rinsed for several minutes in 70% ethanol. The maize SAMs were then peeled off under an anatomical lens. Secondly, the maize SAMs were stained with 20 µg ml^{-1} Hoechst33258 (TaKaRa Biotechnology Company, Dalian, China) at 25 °C for 24 h in darkness. Finally, the morphology of the maize SAM was observed under a Leica TCS-SP2 laser scanning confocal microscope (LEICA, Germany) (Li and Huang, 2005).

Stress and hormone treatments

Zmnf-ya3 mutant and WT seeds were surface sterilized in 10% H_2O_2 for 20 min, washed with distilled water, and then germinated at 28 °C for 2 d in the dark between two layers of moistened filter paper. Uniform germinated seeds were transferred to vermiculite and grown under LD conditions as described above. Uniform seedlings with two leaves were selected and then transferred to 2 litre pots with full-strength Hoagland's nutrient solution (Zhao *et al.*, 2012). The plants were grown in a controlled culture room at 22 °C with a relative humidity of 60%. The photoperiod was 15/9 h, light/dark for LD conditions. The nutrient solution was replaced with fresh solution every 2 d. Seedlings with three leaves were used for stress treatments.

High-temperature stress was carried out by placing three-leaved plants at 40 °C, and seedlings were left in the LD growth conditions as control; the whole treatment lasted for 4 d. For drought treatment, some seedlings were grown in nutrient solution with added 20% polyethylene glycol (PEG) for 1 d, and some seedlings were left in the normal nutrient solution as control (Zheng *et al.*, 2004). The relative water contents (RWCs) of the Zmnf-ya3 mutant and WT were analysed to identify phenotypic differences. Detached leaves were weighed, saturated with water for 24 h, and weighed again, and then dried for 48 h and weighed a third time. The RWC was calculated using the following formula: RWC (%)=[(FM−DM)/(TM−DM)]×100, where FM, DM, and TM refer to the fresh, dry, and turgid masses of the tissue, respectively (Kwasniewski *et al.*, 2016).

For JA treatment, some plants at the V6 stage were placed into 50 mmol l^{-1} JA (Sigma-Aldrich) nutrient solution for 1, 12, or 24 h, and seedlings were left in the normal nutrient solution as a control. For ABA treatment, some plants at the V6 stage were treated with 100 μmol l^{-1} ABA (Sigma-Aldrich) for 24 h, and seedlings were left in the normal nutrient solution as control (Wu *et al.*, 2013). After treatment, leaf7 were sampled for RNA extraction. Three randomly selected plants were pooled together as a biological replicate, with three biological replicates in total.

Real-time reverse transcription–PCR (qRT–PCR)

Total RNA was isolated from the collected samples using TRIzol reagent (Invitrogen, Waltham, MA, USA) and treated with RNase-free DNase I to remove DNA contamination. cDNA was synthesized using a M-MLV reverse transcriptase-based cDNA first-strand synthesis kit (Invitrogen). qRT–PCR was performed using the SYBR® Green CR Master Mix kit (Applied Biosystems, Waltham, MA, USA), following the manufacturer's protocol on a LightCycler® 480II Sequence Detection System. Relative gene expression was calculated according to the $2^{-\Delta\Delta Ct}$ method (Pfaffl, 2001). Expression values were normalized to the *18S* ribosomal gene for qRT–PCR. The primer sequences used in the qRT–PCR assay are listed in Supplementary Table S1.

Results

Phenotypic variation in flowering time and stress responses under LD conditions

The ZmNF-YA3 knock-out mutant (Zmnf-ya3) was obtained through the CRISPR–Cas9 mutagenesis system under the background of Yu658. No significant flowering time differences were observed between Zmnf-ya3 mutant and WT plants under SD conditions (9 h light/15 h dark, 25 °C; Supplementary Fig. S2A, C), whereas Zmnf-ya3 mutant plants flowered on average 4.9 d later than WT plants under LD conditions (15 h light/9 h dark, 25 °C; $P<0.01$; Supplementary Fig. S2B, D). Western blotting analysis showed that NF-YA3 protein was absent from the leaf of Zmnf-ya3 mutant plants but was present in the leaf of WT plants (Supplementary Fig. S2E). These results clearly indicated that ZmNF-YA3 was involved in the regulation of flowering time under LD conditions.

We also noticed that the Zmnf-ya3 mutant and WT plants also differed in drought and heat tolerance under LD conditions (Supplementary Fig. S2F). To investigate the physiological difference of the two genotypes under drought tolerance, RWC determination was conducted by using leaves exposed to drought and heat stresses. The RWC in WT plant leaves (71.6%) was significantly higher than that in the Zmnf-ya3 mutant plants (45.3%) after 1 d drought treatment ($P<0.01$). The RWC in WT plants leaves (61.37%) was also significantly higher than that in the Zmnf-ya3 mutant plants (41.36%) after 4 d heat treatment ($P<0.01$).

Genome-wide analysis of NF-YA3 direct targets in maize

To identify potential genes directly targeted by *NF-YA3*, a ChIP-Seq assay was performed using NF-YA3-specific antibody on chromatin extracted from leaves of V7stage Yu658 plants. The NF-YA3-specific antibody recognizes the full-length NF-YA3 protein from Yu658. Western blotting analysis showed that NF-YA3 protein was absent from the leaf of Zmnf-ya3 mutant plants, but was present in the leaf of Yu658 (Supplementary Fig. S2E). This confirmed that NF-YA3-specific antibody was appropriate for the ChIP experiments. The specificity of the NF-YA3 antibody was determined by using immunoblot analyses on the input (Control). We generated ~4.5 million reads in total (three biological replicates) by using the Illumina platform (50 bp long pair-end reads produced), of which ~3.7 (81%) million reads were uniquely mapped to the maize genome sequence (Supplementary Table S2). NF-YA3-binding sites were predicted using the Model Based Analysis for ChIP-Seq data (MACS2) (q-value <0.05, based on a Poisson distribution). A total of 6624 NF-YA3 peaks identified were distributed across the 10 chromosomes with motifs CCAAG, CTTCGTC, and a core CTTC..C (reverse complement G..GAAG) (Fig. 1A–C). Numerous studies have revealed that NF-YA proteins specifically bind to the CCAAT/G sequence, termed the CCAAT/G-box (Romier *et al.*, 2003; Frontini *et al.*, 2004; Steidl *et al.*, 2004). A total of 2259 peaks (out of 6624) corresponded to 1700 genes, 34.1% of which located in the genic regions as 5 kb upstream of the TSS and 5 kb downstream of the TTS (Fig. 1D, E). Of these 1700 genes, 13.2% are located in the upstream regions (5 kb to +100 bp of the TSS) (Fig. 1E), and genes under two high-scoring ZmNF-YA3 peaks were enriched for Gene Ontology (GO) terms described as responses to stimuli, flower development, regulation of cellular processes, lipid metabolic processes, transcription, and the regulation of gene expression (Supplementary Fig. S3).

Binding motif analysis suggests novel NF-YA3 cis-elements

To explore novel NF-YA3-binding motifs, the 5 kb flanking sequences around the genic peaks were applied to the motif discovery tool (http://meme-suite.org; Machanick and Bailey, 2011), and motif CTTCGTC, with a core CTTC..C (reverse complement GACGAAG), was identified as a statistically defined motif (P=3.2e-085 and P=2.0e-074, respectively; Fig. 1B, C), which was enriched in from −100 bp to 100 bp of genes. *Cis*-element scanning was performed using the CTTCGTC or GACGAAG motifs on the 5 kb flanking sequences around the peak maxima; 426 potential NF-YA3 directly targeted genes with functional annotations were detected. Among the 426 genes, 135 genes in the promoter regions combined with the CTTCGTC motif and contained 15 TFs in the following NF-YA3 target genes (Supplementary

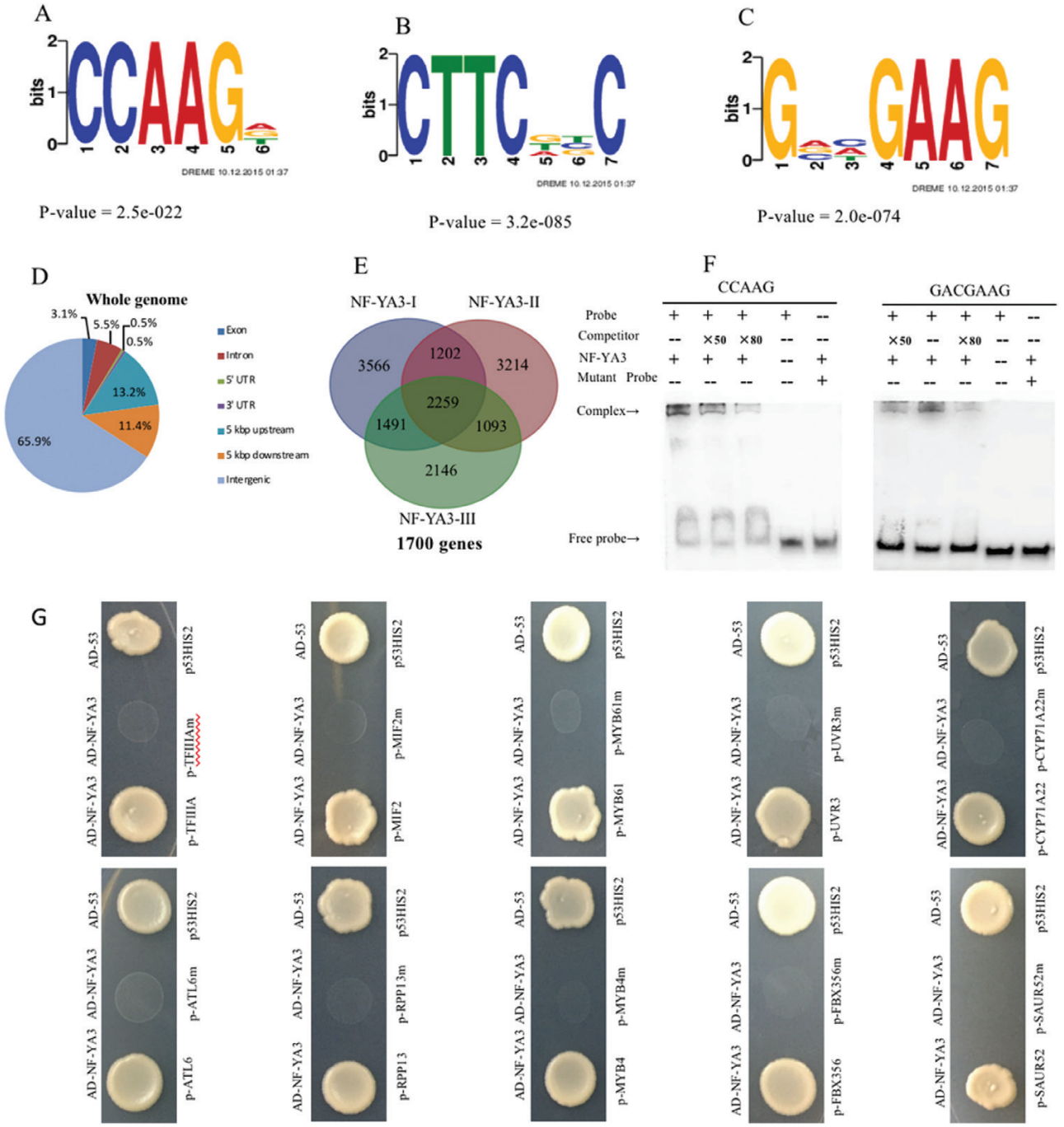

Fig. 1. Summary of ZmNF-YA3 ChIP-Seq results. (A) NF-YA3 binding to CCAAG core motifs identified by MEME-ChIP in the 5 kb flanking sequences around the genic peak summits, and the density plot of this motif. (B) and (C) NF-YA3 binding to a new motif identified by MEME-ChIP in the 5 kb flanking sequences around the genic peak summits, and the density plot of this motif. (D) Distribution of NF-YA3-binding regions in the maize genome. (E) Comparison of NF-YA3-occupied peaks using three biological repetitions. (F) EMSA results confirming the *in vitro* binding of NF-YA3 to CCAAG and GACGAAG. The arrow indicates the position of a protein–DNA complex after the incubation of biotin-labelled DNA probe and the NF-YA3 protein. (G) Yeast one-hybrid assay showing NF-YA3 binding to the new motif. At the top are diagrams of the positive control from p53-AbAi. In the middle are diagrams of negative controls from pMutant-AbAi (mutants from TFIIIA, ATL6, MIF2, RPP13, MYB61, MYB41, FBX356, UVR3, CYP71A22, and SAUR52 promoter fragments, respectively). At the bottom are diagrams of NF-YA3 binding to the CTTC..G motif in the TFIIIA, ATL6, MIF2, RPP13, MYB61, MYB41, FBX356, UVR3, CYP71A22, and SAUR52 promoters, respectively.

Table S3): three zinc finger TFs, two MYB TFs, two leucine-rich repeat (LRR) TFs, a ZF-HD TF, a WD domain TF, an auxin-responsive SAUR protein, an F-box domain-containing protein, an NB-ARC protein, an FAD protein, a cytochrome P450 protein, and a CCT motif-containing protein. To confirm the new NF-YA-binding *cis*-elements, Y1H was performed using a full-length NF-YA3 protein and DNA sequences containing the NF-YA3-binding sites within 200 bp sequences derived from the above-mentioned 10 target genes. An EMSA was performed using a purified NF-YA3 protein and

a labelled DNA probe containing the NF-YA3-binding sites, CTTCGTC and GACGAAG. As shown in Fig. 1F, NF-YA3 bound to CTTCGTC and GACGAAG; the addition of 50× or 80× unlabelled competitor reduced the detected binding of NF-YA3, and it did not bind to mutant probes (CTTCGTC and GACGAAG mutated into CCCCCCT and GGGGAAA, respectively). Without the NF-YA3 protein, no bands were observed, except for the free probe, further confirming the specific binding of NF-YA3 to CTTCGTC and GACGAAG. As shown in Fig. 1G, without the NF-YA3 protein, no interactions were observed. These findings strongly suggested that NF-YA3 bound the novel *cis*-elements through the CTTCGTC or reverse complement GACGAAG motif.

NF-YA3 directly regulates genes related to flower development

Xu *et al.* (2014) found that the miR169 family regulates stress-induced flowering by repressing AtNF-YA, which in turn reduces the expression of Flowering Locus C, allowing the expression of its target genes, such as *FT* and *LEAFY*, to promote flowering in Arabidopsis. Our ChIP-Seq results revealed that NF-YA3 bound to the coding regions of CO-like (GRMZM2G414423, Fig. 2A) and FPF1 (GRMZM2G134941, Fig. 2A), and upstream of ZmFT-like 12 (–3109; GRMZM2G400167, Fig. 2A). Y2H and BiFC results confirmed the interaction of ZmNF-YA3 with CO-like and FPF1 (Fig. 2B). The Y1H result indicated that ZmNF-YA3 bound to the upstream region of ZmFT-Like12 (Fig. 2C). Thus, ZmNF-YA3 may influence flowering time by interacting with the above-mentioned genes.

To understand the effects of *ZmNF-YA3* on *ZmCO-like*, *ZmFPF1*, and *ZmFT-Like12 in vivo*, we measured mRNA levels of the four genes by qRT–PCR in WT, Zmnf-ya3, mutant and Zmft-like12 plants under LD conditions. The ZmNF-YA3 mRNA level was significantly higher in the WT and Zmft-like12 than that in the Zmnf-ya3 mutant in leaf6, leaf7, and leaf8, the ZmFT-Like12 mRNA level was significantly higher in the WT than that in Zmnf-ya3 mutant and Zmft-like12 mutant (Fig. 3A), mRNA levels of CO-like and FPF1 were significantly higher in leaves of the WT than that in Zmnf-ya3 mutant plants under LD conditions (Fig. 3B), and mRNA levels of ZmNF-YA3, CO-like, and FPF1 in leaves were not significanty difference in WT and Zmft-like12 (Fig. 3B). Compared with WT plants, the floral development period of the Zmft-like12 mutant plants was delayed at the V5 stage under LD conditions (Fig. 3C). Combining all the results, we postulated that ZmNF-YA3 promoted floral organ development in maize through interacting with CO-like and FPF1 proteins to form a heterotrimeric complex and binds to the promoter of ZmFT-like12 (Fig. 3D).

NF-YA3 directly regulates a suite of stress response genes

Arabidopsis NF-YA genes are involved in drought, cold, and heat resistance in endoplasmic reticulum stress responses and ABA responses through NF-YB and NF-YC, respectively (Li *et al.*, 2008; Liu and Howell, 2010; Shi *et al.*, 2014). In addition, Alam *et al.* (2015) found that the overexpression of OsHAP2E confers resistance to fungal and bacterial pathogens, as well as to salinity and drought. Our analysis of the ChIP-Seq data revealed a potentially important role for NF-YA3 in the regulation of abiotic and biotic stress response genes in maize (Supplementary Table S4). Abiotic and biotic stress TF genes identified included three *bHLH* genes (*MYC4*, *BHLH92*, and *FMA*), three *MYB* genes (*AtMYB4*, *AtMYB55*, and *GRMZM2G112764*), one *ERF* gene (*CBF2*), one *bZIP* gene (*BZIP45*), one *ZF-HD* gene (*ATHB29*), and one *C2H2* gene (*AC205250.3_FG004*). In addition, other functional proteins involved in the abiotic and biotic stress included four CAMK-related protein kinases, three cytochrome proteins, three heat shock protein chaperones, two regulators of Vps4 activity in the MVB pathway protein, two zinc finger proteins, three NB-ARC domain-containing disease resistance proteins, two pathogenesis-related thaumatin superfamily proteins, one ethanol tolerance protein, one auxin-signalling F-box domain- and LRR-containing protein, and one heavy metal-associated domain-containing protein. These results imply that NF-YA3 may influence the biotic and abiotic stress response through regulating this set of TF genes and proteins.

ZmNF-YA3 responds to abiotic stress by interacting with MYC4 through the JA-induced signalling pathway

MYC4 is an activator of the JA signalling pathway that acts additively with MYC2 specifically to regulate different subsets of the JA-dependent transcriptional responses, and the myc4 mutant showed an enhanced stress resistance through the reduction of bacterial growth (Fernández-Calvo *et al.*, 2011). We noticed that ZmNF-YA3 could also bind to the upstream region of the bHLH TF MYC4 (–1046 bp; GRMZM2G472671; Fig. 4A), which was further supported by Y1H (Fig. 4B). To understand further the regulation mechanism of ZmNF-YA3 in the JA signalling pathway, the WT and Zmnf-ya3 mutant were treated with JA (50 mM JA treatment for 1, 12, or 24 h) at the V6 stage. qRT–PCR results showed that MYC4 was significantly induced after 24 h JA treatment and has a lower expression level in the Zmnf-ya3 mutant than in the WT (Fig. 4C). Thus, ZmNF-YA3 responds to abiotic stress by interaction with MYC4 through the JA signalling pathway.

ZmNF-YA3 responds to abiotic stress by binding bHLHs and bZIPs upstream regions through an ABA-related pathway

As mentioned above, ZmNF-YA3 directly bound to upstream regions of two bHLH TFs, bHLH92 (–1557 bp; GRMZM2G173862;) and FMA (–248 bp; GRMZM2G162450); this was also confirmed by Y1H (Fig. 5A, B). The transcript level of *bHLH92* was highly induced by a wide range of abiotic stresses (such as NaCl, mannitol, dehydration, cold, and heat) and its expression is partially dependent on the ABA biosynthesis pathway (Jiang *et al.* 2009). To understand further the regulation mechanisms

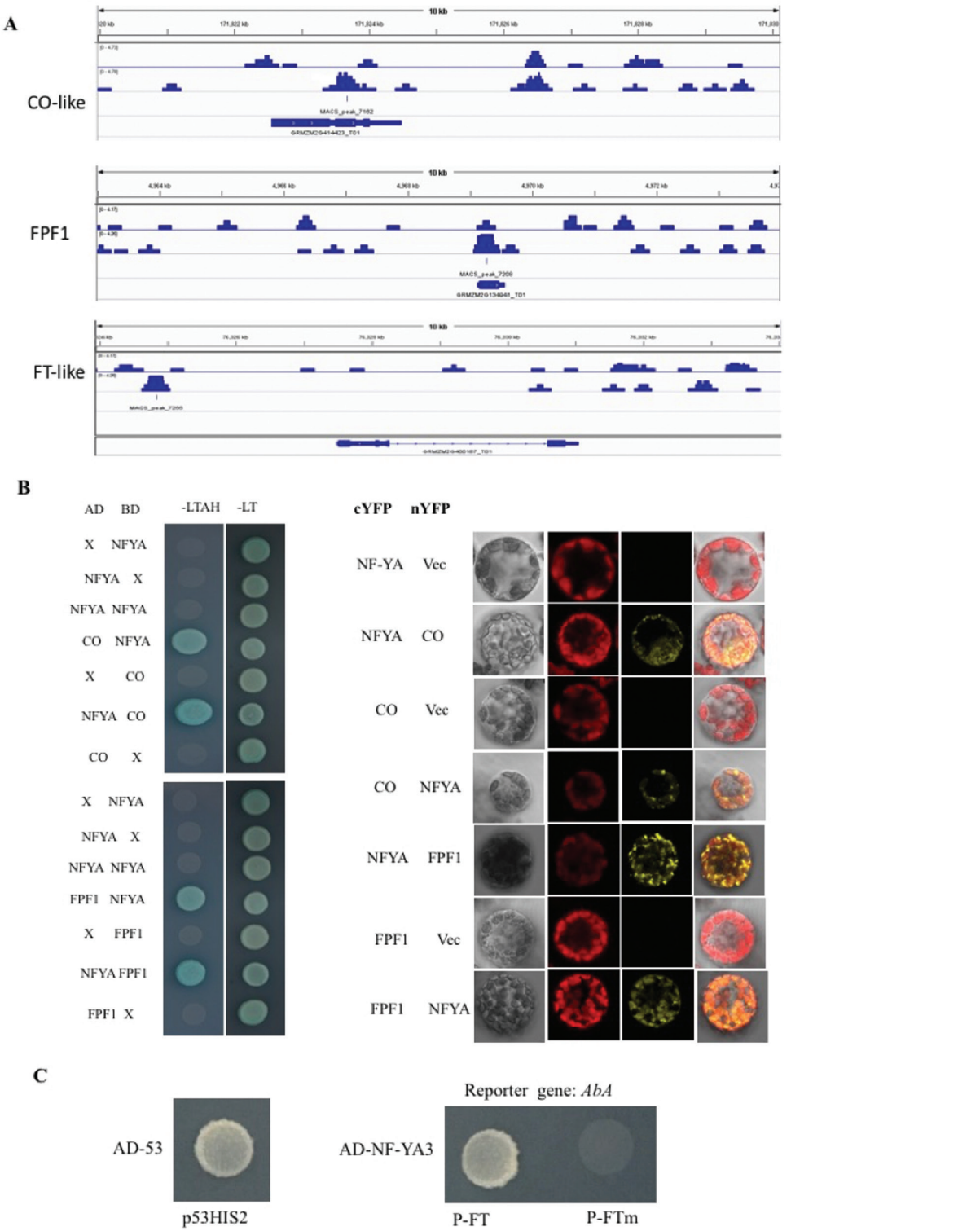

Fig. 2. NF-YA3 interacts with FPF1 and CO-like identified by yeast two-hybrid systems and BiFC, and NF-YA3 binds to FT-like identified by ChIP-Seq and yeast one-hybrid systems. (A) NF-YA3 binding peaks for the positive control genes were shown in the Integrated Genome Brower. For the gene model of ZmCO-like, ZmFPF1, and ZmFT-like, the T01 splicing variant is shown. Large boxes indicate exons. Aligned reads were indicated above (input) and below (ZmCO-like, ZmFPF1, and ZmFT-like) in blue. (B) Yeast two-hybrid (left) and BiFC (right) assay showing NF-YA3 interacting with CO-like (above) and FPF1 (below). Both activation domain (AD) and DNA-binding domain (BD) fusions were generated for NF-YA3, CO-like, and FPF1, and interacted in yeast. Selection media lacking Leu and Trp (-LT) enabled growth, whereas growth in the absence of Ade and His (-LTAH) required the interaction of AD and BD fusions. X indicates an empty vector control. The nYFP–NFYA, CO–cYFP, FPF–cYFP, NFYA–cYFP, nYFP–CO, and nYFP–FPF clones were co-transformed into Arabidopsis protoplasts. NFYA–cYFP, CO–cYFP, FPF–cYFP, and vec–nYFP clones were each also co-transformed into Arabidopsis protoplasts, and represent controls. (C) Yeast one-hybrid assay showing NF-YA3 binding to the promoter *cis*-element of FT-like. On the left is a diagram of the positive control from p53-AbAi. In the middle is a diagram of NY-YA3 binding to the promoter *cis*-element of FT-like. On the right is a diagram of negative controls from pMutant-AbAi (mutant of FT-like promoter fragments).

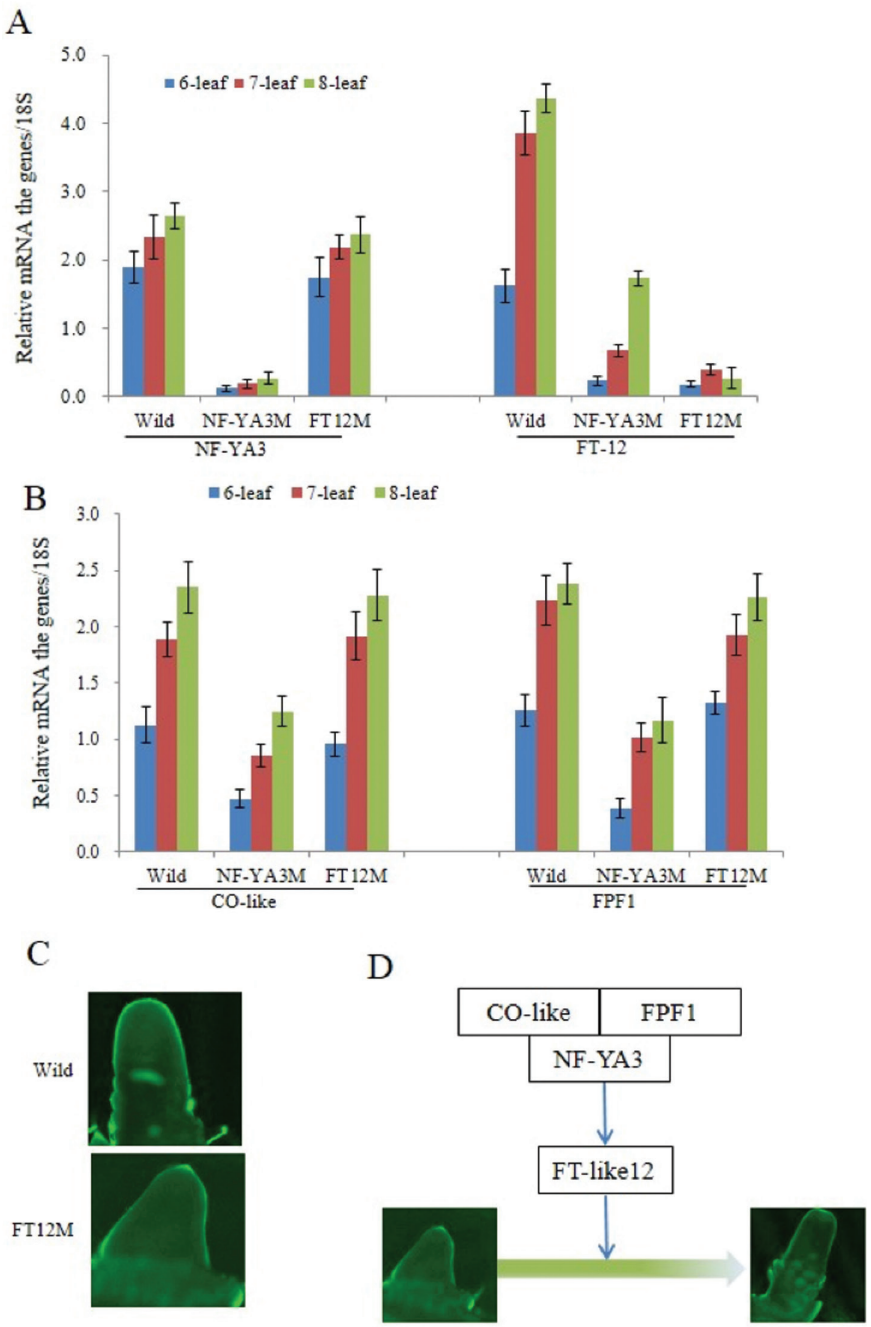

Fig. 3. NF-YA3 promotes flowering by binding the promoter of FT-like. (A) Expression analysis of two expressed genes, NF-YA3 (left) and FT-like (right), among wild-type, Zmnf-ya3, and Zmft-like12 plants using blade tissue from the six-, seven-, and eight-leaf stages under long-day conditions. (B) Expression analysis of two expressed genes, CO-like (left) and FPF1 (right), among wild-type, Zmnf-ya3, and Zmft-like12 plants using blade tissues from the V6, V7, and V8 stages under long-day conditions. (C) Representative SAM morphologies of wild-type and Zmft-like12 plants from the V6 stage under long-day environmental conditions. (D) Schematic model for the floral transition of the shoot apex in maize. Arrows between genes stand for promotion or activation.

of ZmNF-YA3 in the ABA biosynthesis pathway, we treated the WT and Zmnf-ya3 mutant with ABA (100 μM ABA treatment for 24 h) at the V6 stage. qRT–PCR results incidated that expression of bHLH92 was significantly decreased and lower in the WT than in the Zmnf-ya3 mutant after the ABA treatment, and the expression level of FMA was consistent with bHLH92 expression (Fig. 5C).

In addition, bZIPs were reported to be involved in the responses to environmental stresses through the ABA signal transduction pathway (Park *et al*. 2015). We found that ZmNF-YA3 directly bound to one upstream region of the bZIP TF bZIP45, and this was confirmed by Y1H (–855 bp; GRMZM2G174284; Fig. 5A, B). qRT–PCR results showed that the expression level of bZIP45 was increased significantly and was higher in the WT than in the Zmnf-ya3 mutant after ABA treatment (100 μM ABA treatment for 24 h; Fig. 5C). Thus, ZmNF-YA3 responded to abiotic stress

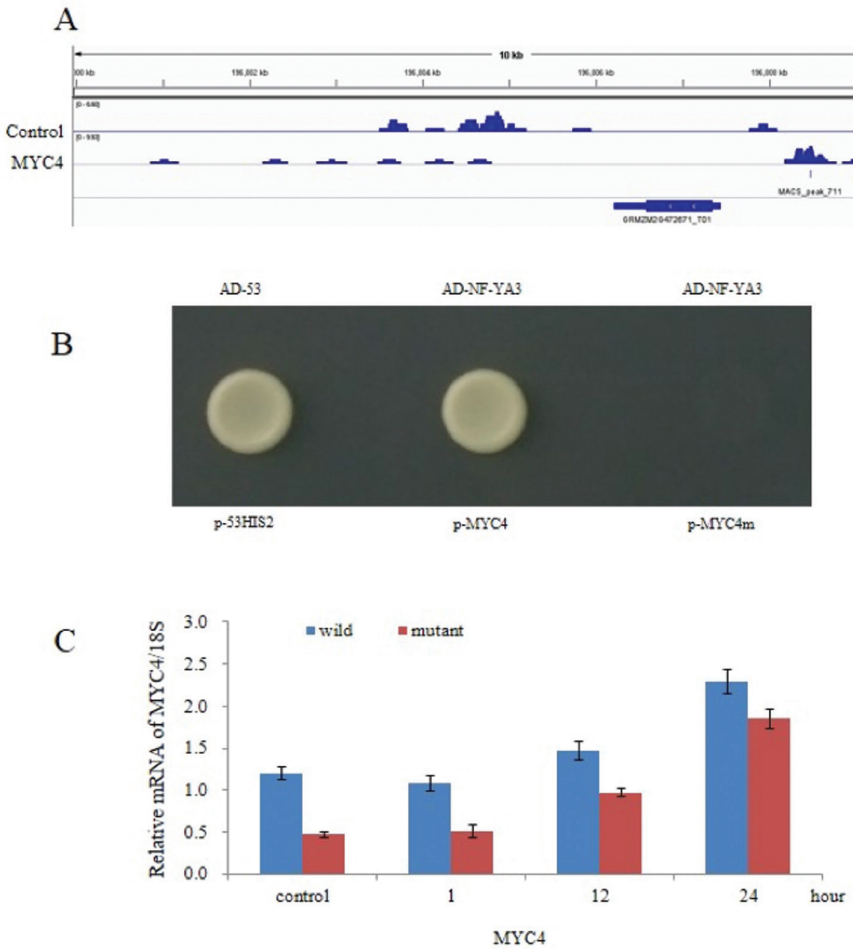

Fig. 4. NF-YA3's binding of the MYC4 promoter in the JA-induced pathway. (A) MYC4's binding peak for the positive control gene is shown in the Integrated Genome Brower. (B) Yeast one-hybrid assay showing NY-YA3 binding to the promoter *cis*-element of MYC4. On the left is a diagram of the positive control from p53-AbAi. In the middle is a diagram of NY-YA3 binding to the promoter *cis*-element of MYC4. On the right are diagrams of negative controls from pMutant-AbAi (mutant of MYC4 promoter fragments). (C) Expression analysis of MYC4 in wild-type and Zmnf-ya3 plants using blade tissue from the six-leaf stage after jasmonic acid treatments of 1, 12, or 24 h under long-day conditions.

by interacting with bHLH and bZIP TFs through an ABA-related pathway.

NF-YA3 directly regulated several development-related genes

Several development-related genes were also detected to be direct NF-YA3 targets, such as those involved in xylem formation, xylem cell differentiation, lateral root formation, and anther development (Supplementary Table S4), of which TF genes included two *C2H2* genes (*GRMZM2G050939*, *TFIIIA*; *GRMZM2G000836*, *WIP4*), one *ZF-HD* gene (*GRMZM2G353076*, *MIF2*), one *bHLH* gene (*GRMZM2G085199*), one *MYB* gene (*GRMZM2G147698*, *MYB61*), one *SBP* gene (*GRMZM2G101499*, *SPL8*), and functional genes including three auxin-responsive SAUR proteins (GRMZM2G346110; GRMZM2G144421; GRMZM2G151656), three zinc-finger proteins (GRMZM2G080139; GRMZM2G082512; GRMZM2G005954), two LRR-containing protein kinases (GRMZM2G450937; GRMZM2G468495), two WD domain-containing proteins (AC207533.2_FG002; GRMZM2G024051), and one heat shock-binding protein (GRMZM2G167868, ERDJ2A). Thus, NF-YA3 could be involved in response to pathogens, and in lateral root, seed coat, and embryo development, as well as pollen germination, by regulating this set of TFs and proteins.

Discussion

NF-Ys are TFs regulating plant development, such as flowering time, stress resistance, and photosynthesis. Up to now, only a limited number of the NF-Y TF family members have been functionally dissected. Most of the research remains at the level of gene cloning, structural characterization, and expression analyses. Little is known about the biological functions of the NF-Y compounds or their downstream targets and upstream regulators. Most of the current studies on the NF-Y TFs are in the model plant *Arabidopsis thaliana*, while their functions in other plants, especially in crop plants, still need to be determined. In this study, ZmNF-YA3 knock-out mutants were obtained using the CRISPR–Cas9-mediated

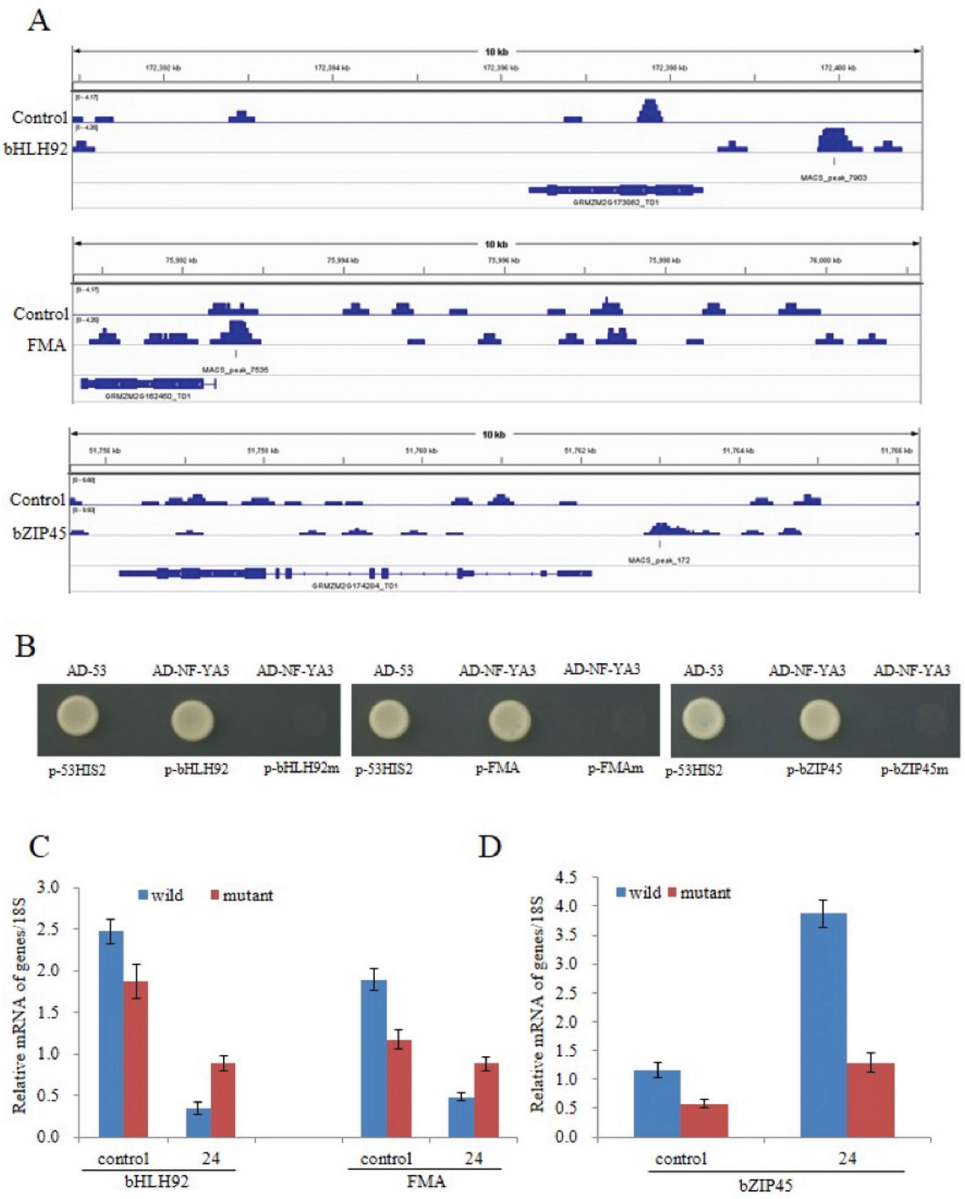

Fig. 5. NF-YA3's binding to bHLH and ZIP promoters is involved in the ABA-induced pathway. (A) bHLH92 (top), FMA (middle), and bZIP45 (bottom) binding peaks for the positive control genes are shown in the Integrated Genome Brower. (B) Yeast one-hybrid assay showing NY-YA3 binding to the promoter *cis*-elements of bHLH92, FMA, and bZIP45. On the left is a diagram of the positive control from p53-AbAi. In the middle is a diagram of NY-YA3 binding to the promoter *cis*-elements of bHLH92, FMA, and bZIP45. On the right are diagrams of negative controls from pMutant-AbAi (mutant of bHLH92, FMA, and bZIP45 promoter fragments). (C) Expression analysis of bHLH92 (left) and FMA (right) in wild-type and Zmnf-ya3 plants using blade tissue from the six-leaf stage after 24 h ABA treatments under long-day conditions. (D) Expression analysis of bZIP45 in wild-type and Zmnf-ya3 plants using blade tissue from the six-leaf stage after 24 h ABA treatments under long-day conditions.

mutagenesis system, and the average flowering time of Zmnf-ya3 was delayed 4.9 d compared with the WT under LD conditions (Supplementary Fig. S2A); abiotic stress (such as drought and high temperature) tolerance was also improved in the Zmnf-ya3 mutant (Supplementary Fig. S2B). ZmNF-YA3 interacted with ZmCO-like and ZmFPF1 to form a complex and bound to the promoter of ZmFT-like12 to promote early flowering, interacted with the JA activator MYC4 to enhance abiotic stress tolerance through the JA signalling pathway, and interacted with bHLH92 and FMA to improve drought and high-temperature tolerance through the ABA-related pathway. These results contribute to a comprehensive understanding about biological function, molecular mechanism, and regulatory networks of NF-Y TFs in maize. At the same time, our results showed that NF-YA3 holds great potential for improvement of agronomic traits and molecular breeding.

ZmNF-YA3 promotes early flowering by binding to the ZmFT-like12 promoter in maize

Photoperiod-dependent flowering is one of several mechanisms used by plants to initiate developmental transition from vegetative to reproductive growth. Photoperiod-dependent species use the relative lengths of day and night to activate or

repress flowering, such that it is timed with the appropriate environmental conditions to maximize reproductive success. NF-Ys are heterotrimeric complexes composed of NF-YA and histone folding domains containing NF-YB/NF-YC. CO interacts with NF-YB and NF-YC subunits to drive the expression of FT in Arabidopsis, which initiates photoperiod-dependent flowering (Ben-Naim *et al.*, 2006; Wenkel *et al.*, 2006; Kumimoto *et al.*, 2008, 2010). In this study, ChIP-Seq and Y2H results indicated that NF-YA3 interacted with CO-like and FPF1 (involved in the gibberellin signalling pathway) to promote expression of ZmFT-like12 in maize to regulate positively flowering time in an FT-dependent manner. This is also consistent with what Siriwardana *et al.* (2016) have reported, namely that NF-YA directly bound to the FT promoter as a positive regulator of flowering in an FT-dependent manner in Arabidopsis. In other species, NF-YB and NF-YC possessed histone-fold motifs that allowed them to form a tight dimer, the crystal structure of which had been determined (Romier *et al.*, 2003). This dimer can then interact with NF-YA and, by analogy with the histone H2A–H2B dimer, binds to DNA non-specifically (Romier *et al.*, 2003). Therefore, we propose that ZmNF-YB and ZmNF-YC proteins should initially form a ZmNF-YB/NF-YC dimeric complex, and then interact with the complex of ZMNF-YA, ZmCO-like, and ZmFPF1 to bind the promoter of ZmFT-like12 to regulate flowering in maize positively. The latest studies also identified that the NF-Y complex interacted with CONSTANS in the photoperiod pathway and DELLAs in the gibberellin pathway (Hou *et al.*, 2014), to bind the promoter of FT directly to regulate flowering time positively in an FT-dependent manner in Arabidopsis (Siriwardana *et al.*, 2016).

ZmNF-YA3 responds to stress through the JA signalling pathway

JAs are lipid-derived signals mediating plant responses to biotic and abiotic stresses. Thus, JAs are widely recognized as regulators of environmental stresses in plants, such as pathogen and pest attack, wounding, ozone exposure, and water deficit (Browse and Howe, 2008). Fernández-Calvo *et al.* (2011) found that the MYC4 protein was required for full responsiveness to JA and suggested that MYC3 and MYC4 co-operated with MYC2 in the positive regulation of JA-regulated genes, such as *VSP2* and *PDF1.2* in Arabidopsis. NF-YA3 bound to MYC4, which is an activator of the JA signalling pathway. MYC4 was significantly induced after a 24 h JA treatment and was down-regulated in the Zmnf-ya3 mutant (Fig. 4B). Thus, ZmNF-YA3 responded to stress by binding to MYC4 through the JA signalling pathway.

ZmNF-YA3 responded to abiotic stress through the ABA-related pathway

ABA is a vital plant hormone and a central regulator that protects plants against abiotic stresses, such as drought and salinity. Members of AP2/ERF, bZIP, zinc finger, NAC, and MYB families, bHLH, and FMA have been frequently reported to be involved in ABA response (Jiang *et al.*, 2009; Jeong *et al.*, 2010, 2013; Park *et al.*, 2015). ZmNF-YA3 directly bound to the promoter regions of two bHLH TFs (bHLH92 and FMA) and one bZIP TF (bZIP45) involved in the ABA-related pathway. bHLH92 and FMA were up-regulated in the Zmnf-ya3 mutant after the ABA treatment (Fig. 5B). bZIP45 was also up-regulated in the Zmnf-ya3 mutant after the ABA treatment. Furthermore, drought and high-temperature tolerance were improved in the WT compared with the Zmnf-ya3 mutant (Supplementary Fig. S2B). These observations are consistent with previous reports that overexpression of OsbZIP46 and OsbZIP72, members of group A, showed ABA responses and improvements in the drought tolerance of rice, respectively. Also in Arabidopsis, expression of seven (out of 13) bZIP TFs is inducible by ABA or abiotic stresses (Lu *et al.*, 2009; Tang *et al.*, 2012). Thus, ZmNF-YA3 improved drought and high-temperature tolerance through the ABA-related pathway.

ZmNF-YA3 might be in plant development

NY-YA has been reported to play important roles in regulating plant growth and development (Ballif *et al.*, 2011; Petroni *et al.*, 2012; Laloum *et al.*, 2013). From the gene ontology analysis, NF-YA3 bound to 17 development-related genes (Supplementary Table S4). For example, *AC207533.2_FG002* is a homologue of *AtRaptor1B*, and *AtRaptor1B* mutants show subtle defects in root and shoot development in Arabidopsis (Anderson and Hanson, 2005). Loss of function of *AtMYB61*, the homologue of *GRMZM2G147698*, resulted in decreassd xylem formation, induced qualitative changes in xylem cell structure, and decreased lateral root formation. In contrast, gain of function of *AtMYB61* has the opposite effects on these traits (Julia *et al.*, 2012). *SPL8* (the homologue of *GRMZM2G101499*), an SBP-box gene, affected pollen sac development in Arabidopsis (Unte *et al.*, 2003). These data imply that NF-YA3 may be involved in plant development through regulation of this set of TFs and proteins.

Conclusion

This work showed that ZmNF-YA3 interacted with ZmCO-like and ZmFPF1 on the protein level to form a complex, and bound to the promoter of ZmFT-like12 *in vivo* to promote early flowering. ZmNF-YA3 also binds to promoters of ZmbHLH92, ZmFAMA, and ZmMYC4 to improve drought and high-temperature tolerance. These results contribute to a comprehensive understanding of the biological functions, molecular mechanisms, and regulatory networks of NF-Y TFs in maize.

Supplementary data

Supplementary data are available at *JXB* online.

Fig. S1. CRISPR–Cas9-mediated mutations of ZmFT-like12 and ZmNF-YA3.

Fig. S2. NF-YA3 phenotypic responses to stress under long-day conditions.

Fig. S3. Gene Ontology analysis of NF-YA3 target genes.

Table S1. Primer sequences used for the experiments.

Table S2. Summary of the sequencing read analysis.

Table S3. Novel NF-YA3 *cis*-elements that bind transcription factor promoters.

Table S4. Stress response and development-related genes regulated by NF-YA3 in maize.

Acknowledgements

This work was supported by grants from the National key research and development plan (2016YFD0101001), the major science and technology project of Henan Province (161100110500-0206), and the Corn Industry Technology System in Henan Province (S2015-02). The authors have no conflicts of interest to declare.

References

Alam MM, Nakamura H, Ichikawa H, *et al*. 2015. Overexpression of OsHAP2E, for a CCAAT-binding factor confers resistance to Cucumber mosaic virus, and Rice necrosis mosaic virus. Journal of General Plant Pathology **81,** 1–10.

Anderson GH, Hanson MR. 2005. The Arabidopsis Mei2 homologue AML1 binds. AtRaptor1B, the plant homologue of a major regulator of eukaryotic cell growth. BMC Plant Biology **5,** 2.

Ballif J, Endo S, Kotani M, MacAdam J, Wu Y. 2011. Over-expression of HAP3b enhances primary root elongation in *Arabidopsis*. Plant Physiology and Biochemistry **49,** 579–583.

Ben-Naim O, Eshed R, Parnis A, Teper-Bamnolker P, Shalit A, Coupland G, Samach A, Lifschitz E. 2006. The CCAAT binding factor can mediate interactions between CONSTANS-like proteins and DNA. The Plant Journal **46,** 462–476.

Browse J, Howe GA. 2008. New weapons and a rapid response against insect attack. Plant Physiology **146,** 832–838.

Fernández-Calvo P, Chini A, Fernández-Barbero G, *et al*. 2011. The Arabidopsis bHLH transcription factors MYC3 and MYC4 are targets of JAZ repressors and act additively with MYC2 in the activation of jasmonate responses. The Plant Cell **23,** 701–715.

Frame BR, Shou H, Chikwamba RK, *et al*. 2002. *Agrobacterium tumefaciens*-mediated transformation of maize embryos using a standard binary vector system. Plant Physiology **129,** 13–22.

Frontini M, Imbriano C, Manni I, Mantovani R. 2004. Cell cycle regulation of NF-YC nuclear localization. Cell Cycle **3,** 217–222.

Fujii H, Chinnusamy V, Rodrigues A, Rubio S, Antoni R, Park SY, Cutler SR, Sheen J, Rodriguez PL, Zhu JK. 2009. In vitro reconstitution of an abscisic acid signalling pathway. Nature **462,** 660–664.

Hirano S. 2012. Western blot analysis. Methods in Molecular Biology **926,** 87–97.

Hou X, Zhou J, Liu C, Liu L, Shen L, Yu H. 2014. Nuclear factor Y-mediated H3K27me3 demethylation of the SOC1 locus orchestrates flowering responses of *Arabidopsis*. Nature Communications **5,** 4601.

Jeong JS, Kim YS, Baek KH, Jung H, Ha SH, Do Choi Y, Kim M, Reuzeau C, Kim JK. 2010. Root-specific expression of OsNAC10 improves drought tolerance and grain yield in rice under field drought conditions. Plant Physiology **153,** 185–197.

Jeong JS, Kim YS, Redillas MC, Jang G, Jung H, Bang SW, Choi YD, Ha SH, Reuzeau C, Kim JK. 2013. OsNAC5 overexpression enlarges root diameter in rice plants leading to enhanced drought tolerance and increased grain yield in the field. Plant Biotechnology Journal **11,** 101–114.

Jiang Y, Yang B, Deyholos MK. 2009. Functional characterization of the Arabidopsis bHLH92 transcription factor in abiotic stress. Molecular Genetics and Genomics **282,** 503–516.

Julia M. Romano, Christian Dubos, Prouse MB, et al. 2012. At MYB61, an R2R3-MYB transcription factor, functions as a pleiotropic regulator via a small gene network. New Phytologist **195,** 774–786.

Kaufmann K, Muiño JM, Østerås M, Farinelli L, Krajewski P, Angenent GC. 2010. Chromatin immunoprecipitation (ChIP) of plant transcription factors followed by sequencing (ChIP-SEQ) or hybridization to whole genome arrays (ChIP-CHIP). Nature Protocols **5,** 457–472.

Ku L, Tian L, Su H, *et al*. 2016. Dual functions of the ZmCCT-associated quantitative trait locus in flowering and stress responses under long-day conditions. BMC Plant Biology **16,** 239.

Kumimoto RW, Adam L, Hymus GJ, Repetti PP, Reuber TL, Marion CM, Hempel FD, Ratcliffe OJ. 2008. The nuclear factor Y subunits NF-YB2 and NF-YB3 play additive roles in the promotion of flowering by inductive long-day photoperiods in *Arabidopsis*. Planta **228,** 709–723.

Kumimoto RW, Siriwardana CL, Gayler KK, Risinger JR, Siefers N, Holt BF 3rd. 2013. NUCLEAR FACTOR Y transcription factors have both opposing and additive roles in ABA-mediated seed germination. PLoS One **8,** e59481.

Kumimoto RW, Zhang Y, Siefers N, Holt BF 3rd. 2010. NF-YC3, NF-YC4 and NF-YC9 are required for CONSTANS-mediated, photoperiod-dependent flowering in *Arabidopsis thaliana*. The Plant Journal **63,** 379–391.

Kwasniewski M, Daszkowska-Golec A, Janiak A, Chwialkowska K, Nowakowska U, Sablok G, Szarejko I. 2016. Transcriptome analysis reveals the role of the root hairs as environmental sensors to maintain plant functions under water-deficiency conditions. Journal of Experimental Botany **67,** 1079–1094.

Laloum T, De Mita S, Gamas P, Baudin M, Niebel A. 2013. CCAAT-box binding transcription factors in plants: Y so many? Trends in Plant Science **18,** 157–166.

Langmead B, Trapnell C, Pop M, Salzberg SL. 2009. Ultrafast and memory-efficient alignment of short DNA sequences to the human genome. Genome Biology **10,** R25.

Lee DK, Kim HI, Jang G, Chung PJ, Jeong JS, Kim YS, Bang SW, Jung H, Choi YD, Kim JK. 2015. The NF-YA transcription factor OsNF-YA7 confers drought stress tolerance of rice in an abscisic acid independent manner. Plant Science **241,** 199–210.

Leyva-González MA, Ibarra-Laclette E, Cruz-Ramírez A, Herrera-Estrella L. 2012. Functional and transcriptome analysis reveals an acclimatization strategy for abiotic stress tolerance mediated by Arabidopsis NF-YA family members. PLoS One **7,** e48138.

Li GP, Huang Q. 2005. Whole stain-clearing technique for observation for pollen grain structure of *Keleteeria fortunei*. Journal of Zhengzhou University (Natural Science Edition) **37,** 44–47.

Li WX, Oono Y, Zhu J, He XJ, Wu JM, Iida K, Lu XY, Cui X, Jin H, Zhu JK. 2008. The *Arabidopsis* NFYA5 transcription factor is regulated transcriptionally and posttranscriptionally to promote drought resistance. The Plant Cell **20,** 2238–2251.

Liu JX, Howell SH. 2010. bZIP28 and NF-Y transcription factors are activated by ER stress and assemble into a transcriptional complex to regulate stress response genes in Arabidopsis. The Plant Cell **22,** 782–796.

Lu G, Gao C, Zheng X, Han B. 2009. Identification of OsbZIP72 as a positive regulator of ABA response and drought tolerance in rice. Planta **229,** 605–615.

Machanick P, Bailey TL. 2011. MEME-ChIP: motif analysis of large DNA datasets. Bioinformatics **27,** 1696–1697.

Merkle T, Leclerc D, Marshallsay C, Nagy F. 1996. A plant in vitro system for the nuclear import of proteins. The Plant Journal **10,** 1177–1186.

Merkle T, Nagy F. 1997. Nuclear import of proteins: putative import factors and development of in vitro import systems in higher plants. Trends in Plant Science **2,** 458–464.

Miyazono K, Miyakawa T, Sawano Y, *et al*. 2009. Structural basis of abscisic acid signalling. Nature **462,** 609–614.

Mu J, Tan H, Hong S, Liang Y, Zuo J. 2013. *Arabidopsis* transcription factor genes NF-YA1, 5, 6, and 9 play redundant roles in male gametogenesis, embryogenesis, and seed development. Molecular Plant **6,** 188–201.

Nelson DE, Repetti PP, Adams TR, *et al*. 2007. Plant nuclear factor Y (NF-Y) B subunits confer drought tolerance and lead to improved corn yields on water-limited acres. Proceedings of the National Academy of Sciences, USA **104,** 16450–16455.

Park SH, Jin SJ, Kang HL, *et al*. 2015. OsbZIP23, and OsbZIP45, members of the rice basic leucine zipper transcription factor family, are involved in drought tolerance. Plant Biotechnology Reports **9,** 89–96.

Petroni K, Kumimoto RW, Gnesutta N, Calvenzani V, Fornari M, Tonelli C, Holt BF 3rd, Mantovani R. 2012. The promiscuous life of plant NUCLEAR FACTOR Y transcription factors. The Plant Cell **24,** 4777–4792.

Pfaffl MW. 2001. A new mathematical model for relative quantification in real-time RT–PCR. Nucleic Acids Research **29,** 2002–2007.

Romano JM, Dubos C, Prouse MB, et al. 2012. At MYB61, an R2R3-MYB transcription factor, functions as a pleiotropic regulator via a small gene network. New Phytologist **195,** 774–786.

Romier C, Cocchiarella F, Mantovani R, Moras D. 2003. The NF-YB/NF-YC structure gives insight into DNA binding and transcription regulation by CCAAT factor NF-Y. Journal of Biological Chemistry **278,** 1336–1345.

Shi H, Ye T, Zhong B, Liu X, Jin R, Chan Z. 2014. AtHAP5A modulates freezing stress resistance in Arabidopsis through binding to CCAAT motif of AtXTH21. New Phytologist **203,** 554–567.

Siriwardana CL, Gnesutta N, Kumimoto RW, Jones DS, Myers ZA, Mantovani R, Holt BF 3rd. 2016. NUCLEAR FACTOR Y, subunit A (NF-YA) proteins positively regulate flowering and act through FLOWERING LOCUS T. PLoS Genetics **12,** e1006496.

Steidl S, Tüncher A, Goda H, Guder C, Papadopoulou N, Kobayashi T, Tsukagoshi N, Kato M, Brakhage AA. 2004. A single subunit of a heterotrimeric CCAAT-binding complex carries a nuclear localization signal: piggy back transport of the pre-assembled complex to the nucleus. Journal of Molecular Biology **342,** 515–524.

Tang N, Zhang H, Li X, Xiao J, Xiong L. 2012. Constitutive activation of transcription factor OsbZIP46 improves drought tolerance in rice. Plant Physiology **158,** 1755–1768.

Unte US, Sorensen AM, Pesaresi P, Gandikota M, Leister D, Saedler H, Huijser P. 2003. SPL8, an SBP-box gene that affects pollen sac development in Arabidopsis. The Plant Cell **15,** 1009–1019.

Walter M, Chaban C, Schütze K, *et al*. 2004. Visualization of protein interactions in living plant cells using bimolecular fluorescence complementation. The Plant Journal **40,** 428–438.

Wenkel S, Turck F, Singer K, Gissot L, Le Gourrierec J, Samach A, Coupland G. 2006. CONSTANS and the CCAAT box binding complex share a functionally important domain and interact to regulate flowering of *Arabidopsis*. The Plant Cell **18,** 2971–2984.

Wu L, Zu X, Wang X, *et al*. 2013. Comparative proteomic analysis of the effects of salicylic acid and abscisic acid on maize (*Zea mays*, L.) leaves. Plant Molecular Biology Reporter **31,** 507–516.

Wu X, Xiong E, Wang W, Scali M, Cresti M. 2014. Universal sample preparation method integrating trichloroacetic acid/acetone precipitation with phenol extraction for crop proteomic analysis. Nature Protocols **9,** 362–374.

Xing HL, Dong L, Wang ZP, Zhang HY, Han CY, Liu B, Wang XC, Chen QJ. 2014. A CRISPR/Cas9 toolkit for multiplex genome editing in plants. BMC Plant Biology **14,** 327.

Xu MY, Zhang L, Li WW, Hu XL, Wang MB, Fan YL, Zhang CY, Wang L. 2014. Stress-induced early flowering is mediated by miR169 in *Arabidopsis thaliana*. Journal of Experimental Botany **65,** 89–101.

Zhang Y, Liu T, Meyer CA, *et al*. 2008. Model-based analysis of ChIP-Seq (MACS). Genome Biology **9,** R137.

Zhao M, Tai H, Sun S, Zhang F, Xu Y, Li WX. 2012. Cloning and characterization of maize. miRNAs involved in responses to nitrogen deficiency. PLoS One **7,** e29669.

Zheng J, Zhao J, Tao Y, *et al*. 2004. Isolation and analysis of water stress induced genes in maize seedlings by subtractive PCR and cDNA macroarray. Plant Molecular Biology **55,** 807–823.